Mon. Not. R. astr. Soc. (1992) **255**, 177–182

Dust in the neutral globules of the Helix nebula, NGC 7293★

J. Meaburn,[1] J. R. Walsh,[2] R. E. S. Clegg,[3] N. A. Walton,[4] D. Taylor[2] and D. S. Berry[1]

[1]*Department of Astronomy, University of Manchester, Oxford Road, Manchester M13 9PL*
[2]*European Southern Observatory, Karl-Schwarzschild-Straße 2, D-8046 Garching bei München, Germany*
[3]*Royal Greenwich Observatory, Madingley Road, Cambridge CB3 0EZ*
[4]*University College London, Gower Street, London WC1E 6BT*

Accepted 1991 October 1. Received 1991 September 25; in original form 1991 June 7

SUMMARY

Images of the ionized knots and spokes within the helical structure of the Helix nebula have been obtained with subarcsecond resolution in the light of the Hα + [N II], [O III] 5007 Å and [O II] 3727 Å emission lines. The [O III] image reveals the knots and their tails in absorption. The globules and tails must be dusty and are seen against the diffuse, central [O III]-emitting volume of the Helix nebula. The curved heads of these neutral knots are radiatively ionized by the light of the central star to produce spatially resolved, bow-shaped Hα + [N II] and [O II]-emitting structures displaced (measured for the most prominent globule) by 1.65 arcsec (3.1×10^{15} cm) towards the central star from the peak of the absorption. Assuming a standard interstellar dust/gas ratio and reddening laws, we find that the total mass in one globule is $\geq 1.0 \times 10^{-5}\ M_{\odot}$ and the mean gas density $N_{\rm H}$ is 6.2×10^{5} cm^{-3}. Considerations on the nature and survival of the globules and their tails are also discussed.

1 INTRODUCTION

The Helix nebula (NGC 7293, PK 36 − 57°1) is probably the closest planetary nebula with a distance of only ≈ 130 pc (Cahn & Kaler 1971; Acker 1978; Daub 1982). Its prominent helical structure is of low ionization and the observed extensive CO (Huggins & Healey 1986) and H_2 (Storey 1984) emission implies the existence of a substantial quantity of cool, molecular gas, perhaps in the form of dense, shielded clumps. The helical features surround two approximately spherical shells of highly ionized gas in the nebular core which emit strongly in the [O III] 5007 Å line and are expanding radially at about 20 km s^{-1} (Meaburn & White 1982). A faint, low-ionization filament forms a halo to the whole complex (Walsh & Meaburn 1987).

Perhaps the most interesting features within the Helix nebula are the ionized knots, ≈ 1 arcsec across, with cometary-like tails (Vorontsov-Velyaminov 1968) which form radial filaments pointing away from the central star. They are found on the inside edge of the prominent helical structure and on the outer edge of the inner, highly ionized core.

The nature of these knots was discussed earlier by Kirkpatrick (1972), Van Blerkom & Arny (1972), and Capriotti (1973). Capriotti ascribed their formation to a Rayleigh–Taylor instability at the inner edge of the main planetary-nebula gas shell, and predicted that their 'heads' would have a radius 7×10^{14} cm and a mass 2×10^{27} g ($7 \times 10^{-7}\ M_{\odot}$) at their time of formation. Kirkpatrick and Van Blerkom & Arny interpreted the 'tails', pointing radially away from the heads, as shadow regions shielded from the central star's UV radiation, and thus having a lower electron temperature and higher density than the diffuse, surrounding gas. More recently, Dyson *et al.* (1989) suggested that the visible knot 'heads' are ionized skins around cold, dense, molecular globules which have their origin in the SiO maser spots which formed in the atmosphere of the central star during its red giant phase and survived the ejection of the nebula.

The neutral component in both the knots and their long tails has now been indicated in an unexpected way. Hα + [N II] images obtained at high spatial resolution have resolved the bright apices of these low-ionization knots as well as their faint tails. Similar images in the light of the [O III] 5007 Å emission line reveal the presence of dusty absorbing cores to both the knots and their tails, for they are located on the near side of the [O III]-emitting nebular core and are themselves remarkably faint in [O III] emission.

2 OBSERVATIONS AND RESULTS

Images of NGC 7293 were obtained on the night of 1990 July 25 on the ESO 3.5-m New Technology Telescope using EFOSC2 (Eckert, Hofstadt & Melnick 1989) with a blue

★ Based on observations made at the European Southern Observatory (ESO), La Silla, Chile.

coated Thompson 1024 square CCD [type TH 31156, see D'Odorico (1990)] as detector. The filters used were Hα + [N II] of half-width 63 Å, an [O III]5007 Å filter 66 Å wide, and an [O II]3727 Å (central wavelength 3777 Å) of width 100 Å. The field centre was $22^h26^m52^s$, $-21°02'30''$ (B1950), to the north of our adopted position of the central star ($22^h26^m54^s.7$ $-21°05'37''$). The plate scale was 0.152 arcsec per pixel, but we used on-chip binning to obtain a 512×512 array with a scale of 0.304 arcsec per pixel. The resultant 156×156 arcsec^2 field is marked against some contours of [N II] of NGC 7293 [from an image through a 10 Å bandwidth filter – see Meaburn & White (1982)] in Fig. 1. The measured width at half peak intensity of the stellar images is 0.86 arcsec. The exposure times were 900 s for the Hα + [N II], [O III] and [O II] images. The data have been bias-subtracted, cleaned of cosmic rays and flat-fielded. The Hα + [N II] and [O III] images are shown in Plates 1(a) and (b), respectively. The [O II] image was weak so was not extensively analysed. The absolute surface brightnesses (erg s^{-1} cm^{-2} sr^{-1}) in the emission lines were estimated (approx. ± 30 per cent accuracy) by calculating the throughput of the atmosphere, telescope and filter and the photon response of the detector using many of the parameters measured during the commissioning of the instrument. Small corrections for sky light were applied to all results.

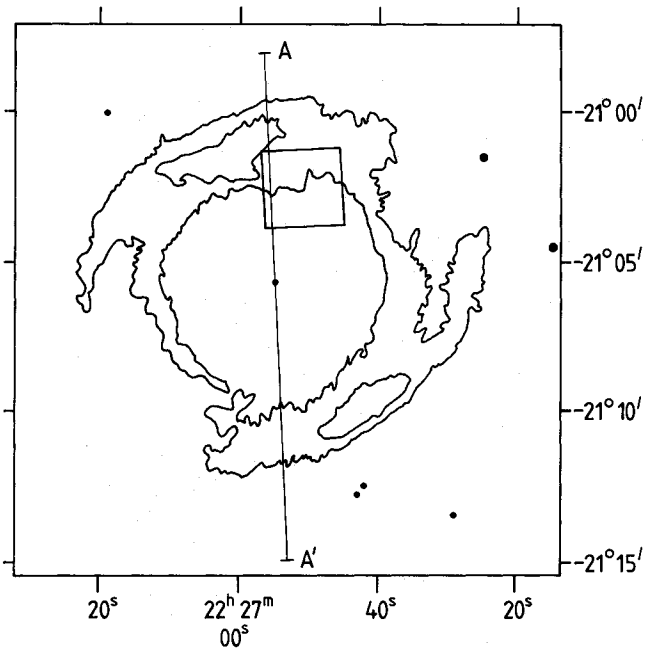

Figure 1. The field of view for Plates 1(a) and (b) is shown as a box against some of the contours of the [N II] emission from the bright helical structure of the Helix nebula. The line AA′ marks the cut in Fig. 2.

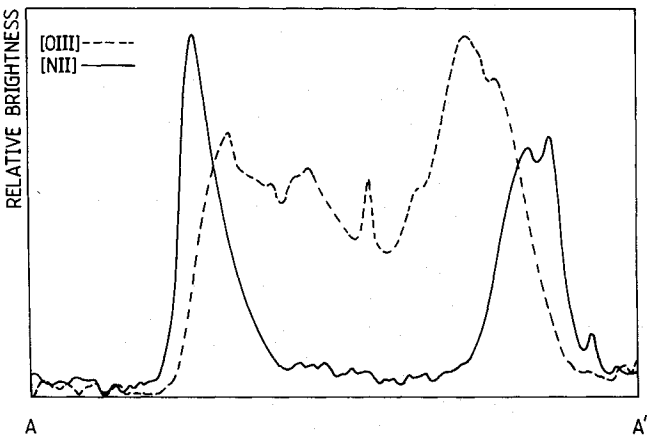

Figure 2. The variations in relative brightness of the [N II]6584 Å and [O III]5007 Å lines along the path marked AA′ in Fig. 1 are shown. The blue central star is seen as a spike on the [O III] curve only. [The data here are from Meaburn & White (1982).]

Enlargements of the Hα + [N II] and [O III] images of the most prominent knot and tail within this field are shown in Plates 2(a) and (b), respectively. This knot is located 194 arcsec north of the central star, or about 0.122 pc for our adopted distance of 130 pc to the nebula. That this knot exists on the interface between the bright low-ionized helical structure and the inner [O III]-emitting core is illustrated in Fig. 2. Here the brightnesses of the [N II]6584 Å and [O III]5007 Å lines are compared along the cut marked AA′ in Fig. 1 (data from Meaburn & White 1982).

The contours of equal Hα + [N II] brightness from the present data are compared in Fig. 3 with those for [O III] for the head of the knot shown in Plates 2(a) and (b). Brightness

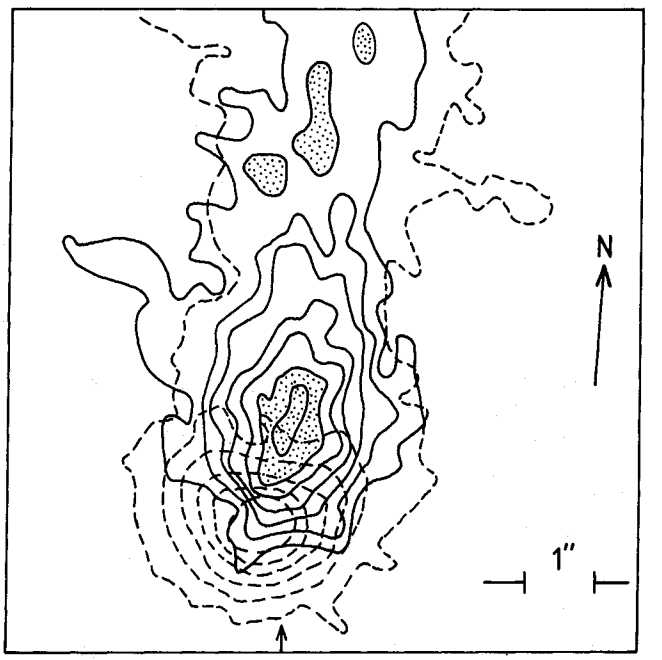

Figure 3. Contours of equal surface brightness in the Hα + [N II] lines, with linear intervals, of the head of the knot shown in Plate 2(a), are shown by dashed lines. (The highest contour is at 6.6×10^{-5} and lowest at 2.6×10^{-5} erg s^{-1} cm^{-2} sr^{-1}.) Those for the [O III]5007 Å line of the same region (Plate 2b) are shown as solid contours. This data array has been corrected, before contouring, for the overall slope across the field of the [O III] surface brightness so that the full extent of the dark absorption features can be depicted. Local minima in the resultant [O III] contour map are shaded. The half-power beamwidth of the seeing disc is also shown. The arrowed line shows the position of the cut for Fig. 4. The lowest [O III] contour represents 40.3 per cent absorption. The peak Hα + [N II] brightness is centred (± 1 arcsec) on RA: $22^h26^m54^s.0$ and Dec: $-21°03'23''$ (B1950 coordinates) – by measuring a UK Schmidt IIIaF plate to ± 1 arcsec accuracy using the surrounding star field for positional reference.

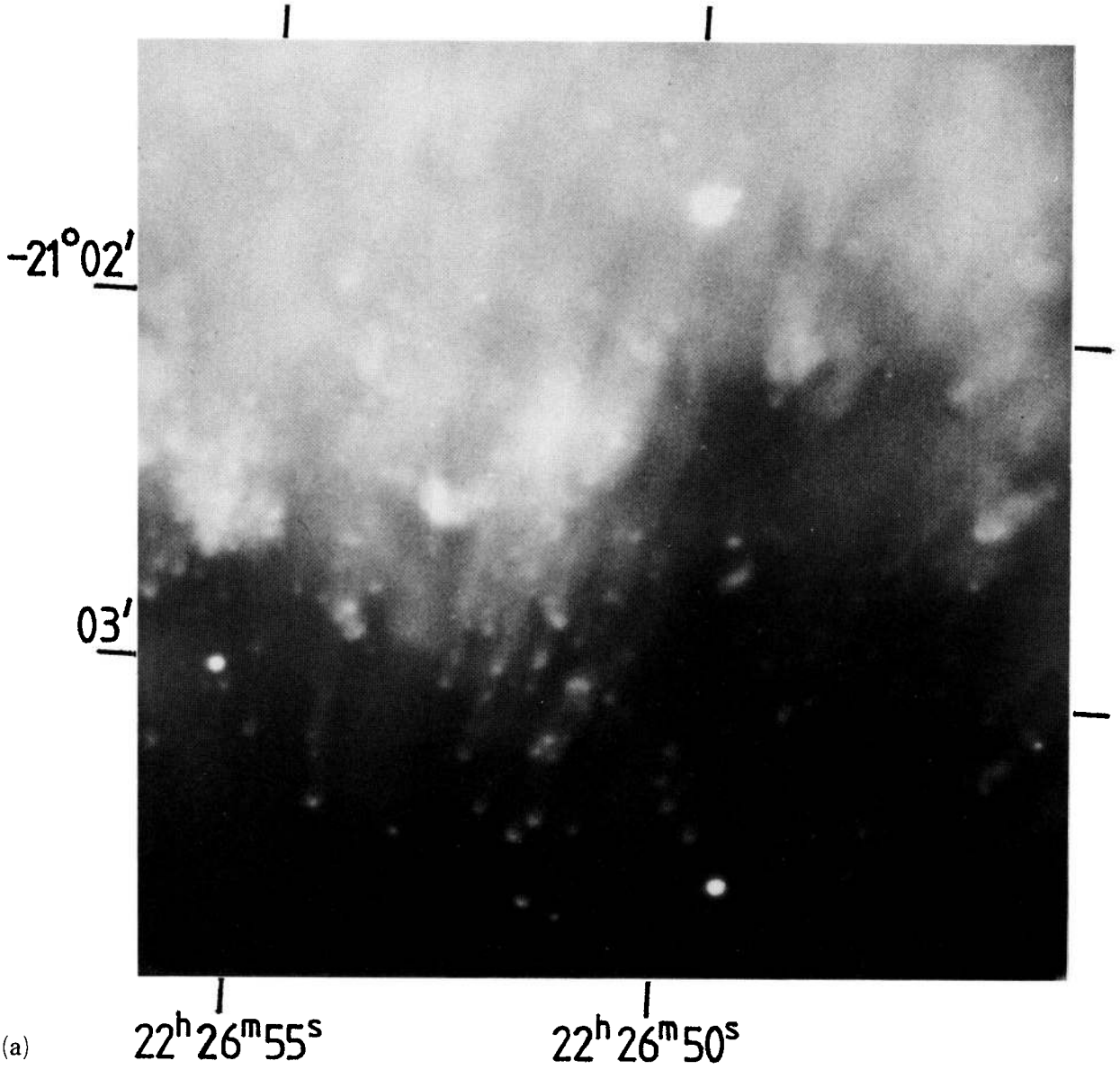

Plate 1. (a) A positive print of the CCD data array for the whole field marked as a box in Fig. 1 in the light of Hα + [N II]. (b) As for (a) but in the light of [O III].

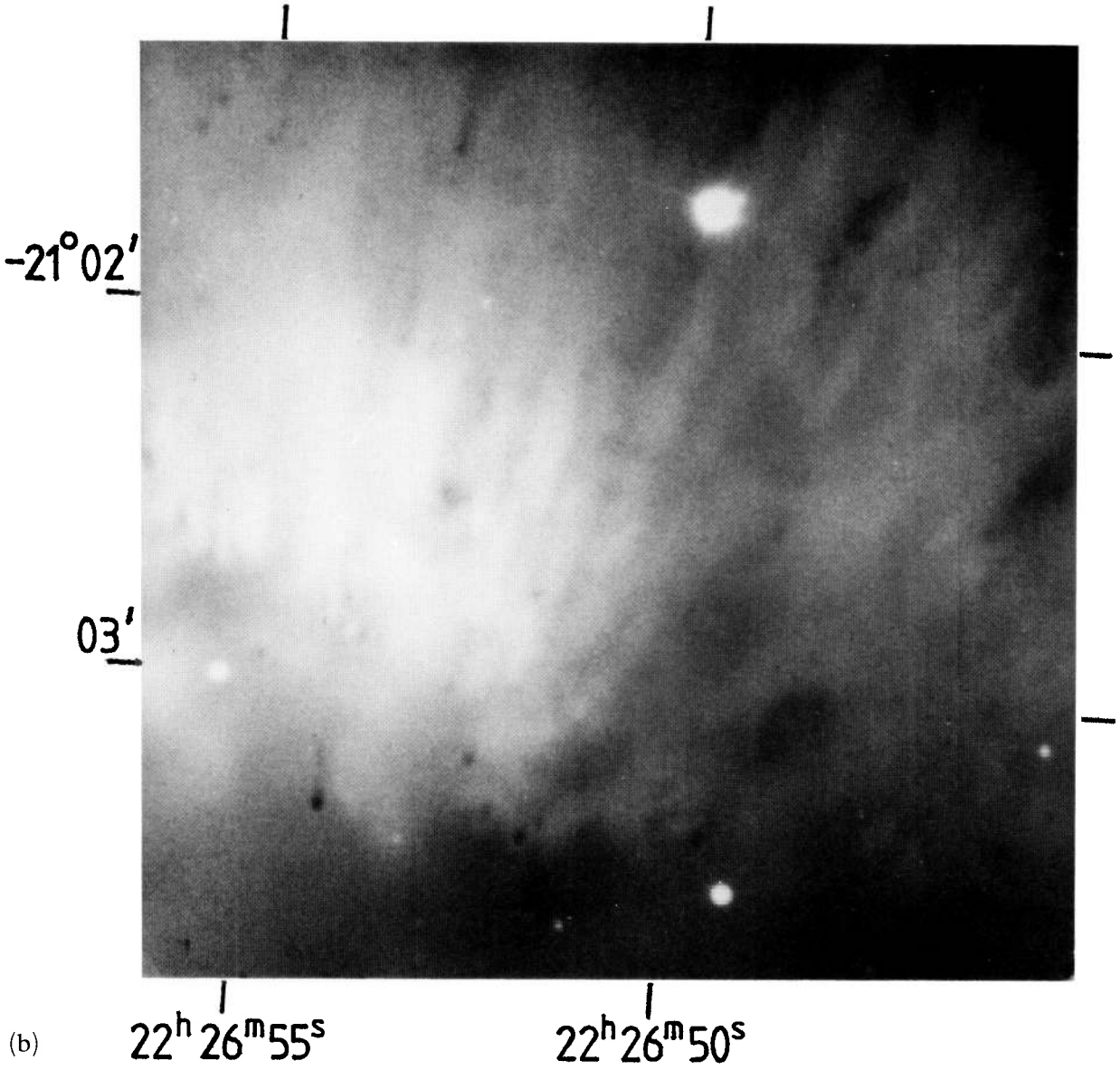

(b)

Plate 1 – *continued*

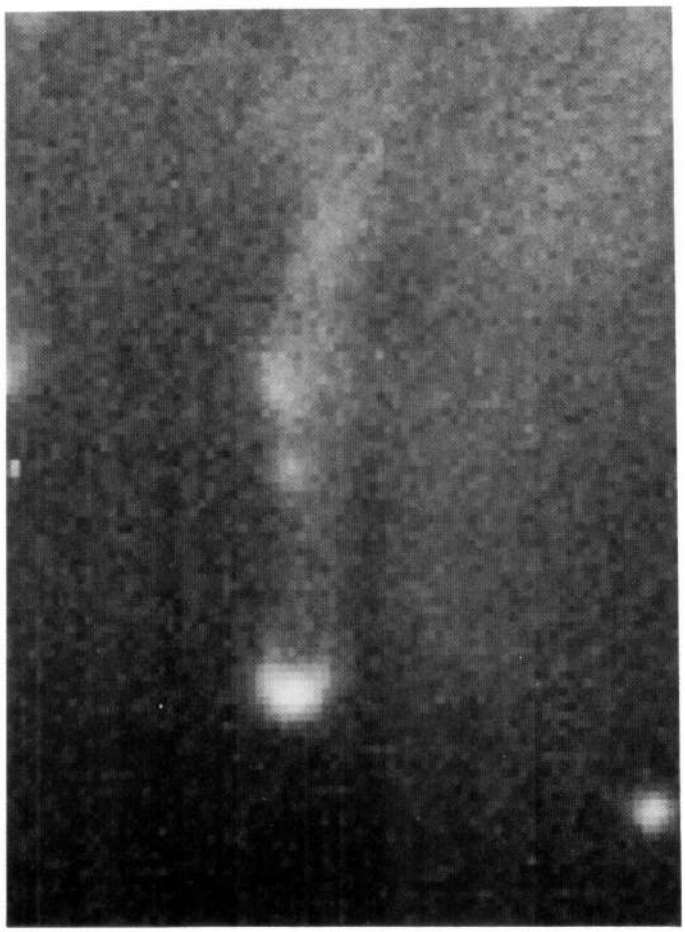

Plate 2. (a) An enlargement in the light of Hα + [N II] of the most prominent knot and tail seen in the field shown in Plate 1. (b) As for (a) but in the light of [O III] from the array shown in Plate 1(b).

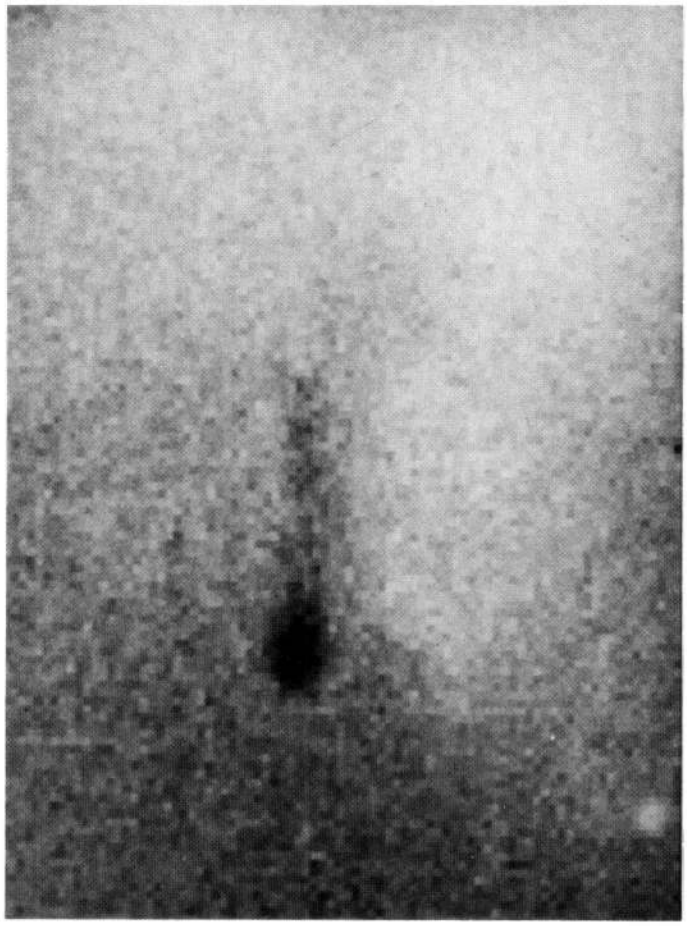

(b)

Plate 2 – *continued*

cuts along a north–south line (marked in Fig. 3) are shown in Fig. 4. The bow-shaped structure at the head of the knot is emphasized in the deconvolved array which is contoured in Fig. 5. A maximum-entropy deconvolution technique based on the MEMSYS3 package produced by Gull and Skilling (Skilling 1989; Gull 1989) was used to increase the effective angular resolution from the 0.86 arcsec which was determined by the seeing disc to ≈0.5 arcsec permitted by the noise level.

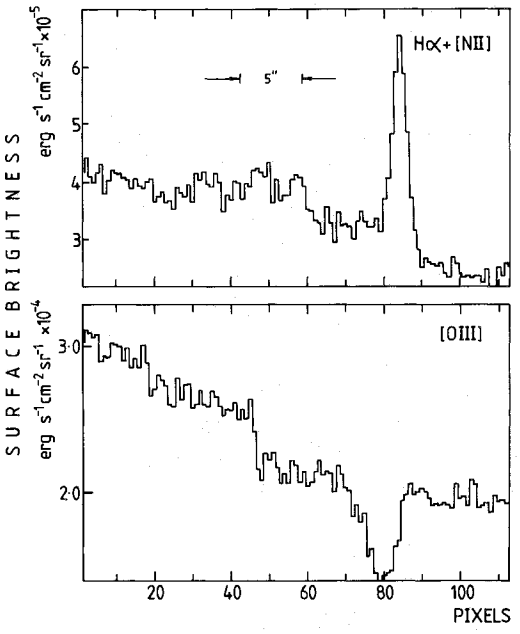

Figure 4. The variations in surface brightnesses of the Hα + [N II] and [O III] emission lines along the north–south line marked in Fig. 3 through the head of the knot in Plates 2(a) and (b) are shown. The length of this cut equals the full height covered by the enlargement in Plates 2(a) and (b). No correction has been made for the slope of the [O III] brightness across the field in this case.

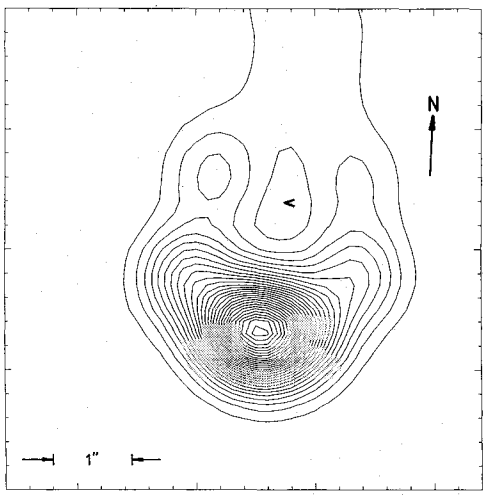

Figure 5. Contours with linear intervals of equal surface brightness of the Hα + [N II] emission from the deconvolved array of the head of the ionized knot shown in Plate 2(a). The highest contour is at 1.1×10^{-4} and the lowest at 2.6×10^{-5} erg s^{-1} cm^{-2} sr^{-1}

3 DISCUSSION

3.1 Basic parameters for globules

Many of the knots with long tails are seen in Plate 1(a) to be emitting Hα + [N II] but absorbing the background [O III] emission strongly (Plate 2b). We interpret the absorption as due to dust, both in the knots and their tails. The bright ionized head of the most prominent knot and tail [Plates 2(a) and (b), Figs 3 and 4] forms an arc around the absorbing material and is displaced by 1.65 arcsec (3.1×10^{15} cm) upstream of the strongest absorption in the neutral globule towards the ionizing star. Evidence for a dusty, neutral component in the core of the tail can also be seen in Plate 1(b), Plate 2(b), and Fig. 3, for the absorption of the [O III] light is elongated northward from the bright Hα + [N II] emissive head of the knot. The sky background in the filter passbands could not be determined since the whole CCD field is filled by emission. Offset exposures in the field of the planetary nebula IC 418 were examined and after correcting for the differing airmasses the estimated sky background was subtracted from the Helix frames.

Although the [O II] image is weak, we were able to measure the positions of the emission knots and compare them with those seen in the Hα + [N II] frame. After correction for misregistration of the two frames made from measured stellar positions, we found for four knots that the emission coincides to within about ±2 pixels (0.6 arcsec). This suggests that the [N II] emission in the ionized head may be stronger than Hα, and does confirm that the bow shape seen is emitting in low-excitation lines. For 15 knots selected as being bright and on a low background (hence closest to the central star), the positions and strength of the peak emission on the Hα + [N II] frame and the peak absorption on the [O III] frame were measured. For five of these globules no [O III] absorption could be detected; it is noteworthy that these mostly lie to the west of the field. Of the 10 globules with measured Hα + [N III] and [O III] positions, the mean displacement is 0.9 ± 0.3 arcsec and the range is 0.4 to 1.4 arcsec. The mean width was 1.8 (±0.1) arcsec. Also measured was the extent of the bow structure along a line perpendicular to the direction to the central star. The mean width was 1.8 (±0.1) arcsec (range 1.4 to 2.5 arcsec). There appeared to be no correlation between the width of the bow structure and the displacement between the emission and absorption peaks, nor any correlation between the displacement and the [O III] absorption strength. However there was a significant correlation for the displacement between the emission and absorption peaks and the strength of Hα + [N II] emission.

The 1.63-arcsec observed east–west width of the most prominent absorbing globule is resolved by the 0.86-arcsec seeing disc (see Fig. 3) to give a corrected width of 1.36 arcsec. The 34 per cent observed depth of the strongest absorption feature increases to 40.3 per cent if the same correction for seeing is made and a sky background correction is applied. These percentages are complicated by the possible presence of some foreground [O III] emission in which case 40.3 per cent represents a lower limit to the percentage of the absorption that is occurring. The peak visual interstellar extinction caused by the gas in this one globule is then $A_V \geq 0.49$ mag to give $E(B-V) = 0.158$ mag assuming the normal interstellar reddening law with $R = 3.1$ (Seaton 1979).

The mean gas density, N_H, and the total interstellar mass, M_g, of this globule can then be estimated if the gas/dust mass ratio is the same as in the general interstellar medium, in which case (Bohlin, Savage & Drake 1978)

$$N(H+H_2)/E(B-V) = 5.8\times10^{21} \text{ atoms cm}^{-2} \text{ mag}^{-1} \quad (1)$$

and Hildebrand (1983) gives:

$$M_g = 5.8\times10^{21}\, E(B-V)\, D^2 m\mu \times \text{projected area}, \quad (2)$$

where D is the distance, m the mass of a proton and μ is the average atomic mass number (here taken to be 1.35). For the 1.36×2 arcsec^2 globule with ≥ 40.3 per cent absorption, from equations (1) and (2), its mass $M_g \geq 1.0\times10^{-5}\, M_\odot$ and its atomic plus molecular (i.e. H I and H_2) mean density $N_H \geq 6.2\times10^5$ cm^{-3}. (Note that the range of distances D given in the literature for NGC 7293 is about a factor of 2 and this basic uncertainty dominates all others in the estimation of the parameters of this globule.)

We searched for excess [O III] emission from the heads and tails of all the globules seen on Plate 1, but found none. This seems surprising, as one might expect some gas at densities $N_e \sim 200$–1000 cm^{-3} (intermediate between the smooth background gas at 50 cm^{-3} and the knot core at $N_e > 10\,000$ cm^{-3}) in a halo around the knot. One possibility is that these knots are all located just outside the nebula's He^+ Strömgren sphere, so that the photon field for $h\nu > 24$ eV is attenuated and no O^{++} ions are present. Certainly, Fig. 2 shows that the knots are typically located between the O^{++} and N^+ zones of the nebula. The amount of foreground [O III] 5007 Å light over the absorbing core of the knot may then be negligible, in which case the lower limits to the calculations of M_g and N_H may apply. However, a difficulty with this picture is that the H Strömgren sphere is predicted by models to lie inside or at the He Strömgren sphere, so that no O^+ or N^+ ions would exist either, these having become neutral along with the hydrogen.

An alternative is that there is indeed very little gas at the intermediate densities mentioned above, with a rapid transition from the low-density background gas to the dense knot. (Calculations show that, at the adopted distance from the central star, gas with $N_e \gtrsim 1000$ cm^{-3} has O only in the form O^+ and not O^{++}.) Any intermediate-density gas behind the knot may be in the knot's shadow, which is predicted to contain only lower stage ions (Section 1).

The gas-to-dust ratio inside the globule is unknown, and could be markedly different from the typical value for diffuse clouds. On the one hand, the dust might have formed in the dense globule in the red giant atmosphere, and now be mixed with more atomic and molecular hydrogen, lowering the ratio. On the other hand, conditions inside the globule's core [$N_H \sim 10^6$ cm^{-3} from the present measurements and $T \simeq 10$ K suggested by Dyson *et al.* (1989)] might have favoured the condensation of many solids, which would increase the ratio. There are around 60 globules of this nature apparent on the Hα + [N II] image alone. Assuming 10 such fields around the inner perimeter of the bright helical shell in NGC 7293 suggests a total mass within them of $\approx 6\times10^{-3}\, M_\odot$. This is around 100 times less than the total neutral mass implied by the observations of far-infrared emission made by Leene & Pottasch (1987). However, there are very large uncertainties in deducing this total mass from the far-infrared emission.

The cometary tails to the knots are interesting in their own right. The one depicted in Fig. 3 also has a dusty, cylindrical core, pointing diametrically away from the central star. Around 7 per cent of the background [O III] emission is absorbed (see Fig. 4) through the centre of the tail to give $A_V = 0.07$ mag of absorption and $E(B-V) = 0.03$ mag in which case, from equation (1), the mean H I and H_2 density of the tail is $N_H = 5.6\times10^4$ cm^{-3} with all the same reservations as the calculations for its globular head. Although this is a small percentage of absorption the absorbing area extends over a large area (see Plate 2b) which permits its estimation to ± 2 per cent accuracy limited by the accuracy of the sky background subtraction.

3.2 Models

Dyson *et al.* (1989) suggested that the globules in NGC 7293 formed in the red giant's atmosphere. The globules must then be massive enough to have survived the mass-loss phases in the formation of the planetary nebula. The elongated shape of the neutral core of the globule shown in Plate 2(b) and Fig. 3 suggests that, whatever its origin, it has been significantly modified by the particle winds that have swept past in its lifetime.

Radiative ionization by hard photons from the central star could produce on its own the crescent-shaped ionized head of the globule shown in Fig. 5. If a supersonic particle wind is currently interacting with this globule a bow shock will also be present. Additional heating and even further ionization (depending on the wind speed) of the emitting head of the globule will be occurring as a consequence. It is interesting that the shape of the Hα + [N II] head of the globule shown in Fig. 5 is very similar to that modelled for the interaction of a shock with a gas cloud by Nittman, Falle & Gaskell (1982) although in reality radiative ionization must complicate such a simplistic model.

The variation in the relative strengths of the [O III] absorption and the Hα + [N II] emission shown by the 15 globules is best understood if the globules are distributed with depth, such that bright ones with no absorption are those at the rear edge of the [O III]-emitting region. The displacement of the emission and absorption peaks depends on the angle between the line joining the globule to the central star (i.e., the axis of the flow around the globule) and the observer's line of sight. That the displacement depends on the strength of Hα + [N II] emission follows from the larger depth of ionizing gas at the head of the globule when viewed perpendicular to the axis of the globule flow.

A working hypothesis is that all the globules are of similar size but higher spatial resolution data are required to test this point. However, the width of the bow structures does not display much variation indicating some confirmation for similar size. Clearly the best view is obtained when the line joining the globule to the star is perpendicular to the line of sight and the globule is between the O^{++} zone and the observer. In this case the absorption is strongest, the displacement between emission and absorption peaks is largest and the emitting depth of gas is greatest. This is most probably the case for the globule chosen to be analysed and shown in Plates 2(a) and (b).

Previous work (Kirkpatrick 1972; Van Blerkom & Arny 1972) concentrated on interpreting the cometary tails to the

Helix knots as part of the diffuse background gas shadowed from the central star. This suggestion is very plausible. However, another possibility is now worth exploring in the light of more recent understanding of the interactions of stellar winds with the surrounding interstellar medium. The tails could represent photoionized gas which has been blown off the surfaces of the globules by successive winds (pulling the dust with them).

3.3 Wind-formed globule tails

The plausibility of forming the tails by winds can be illustrated quantitatively, by consideration of the lifetimes of the neutral and ionized components of a globule in a supersonic wind. The equation of motion of a gas cloud of density N_H and radius r, subjected to a wind of density n_w and velocity v_w is

$$\frac{dv}{dt} \approx \frac{3}{4}\frac{n_w}{N_H}\frac{v_w^2}{r}.$$

The ram pressure will produce a pressure difference across the cloud of the order $n_w v_w^2$, resulting in an expansion of the cloud at the associated sound speed

$$\frac{dr}{dt} \approx \gamma\left(\frac{n_w}{N_H}\right)^{1/2} v_w$$

(Nittman *et al.* 1982). The cloud will not remain spherically symmetric and homogeneous throughout its expansion, so N_H and r must represent some average density and radius respectively. If $N_H r^3$ is constant, integration of the equation of motion yields

$$t(r) \approx \frac{2}{\gamma^{1/2}}\frac{r_0}{v_w}\left(\frac{N_H'}{n_w}\right)^{1/2}\left[1-\left(\frac{r_0}{r}\right)^{1/2}\right],$$

where r_0 and N_H' are the initial values of the radius and density. Thus, assuming $r \gg r_0$, the lifetime of the cloud is of the order

$$t \sim \frac{r_0}{v_w}\left(\frac{N_H'}{n_w}\right)^{1/2}.$$

We now apply this to the globules of NGC 7293. If the temperatures of the neutral and ionized globule material are respectively T_n and T_i, then, assuming pressure equilibrium, the density of the ionized gas is $n_i = N_H(T_n/T_i)$, where N_H is the neutral globule density. The time-scale for the disruption of the ionized component is then $t_i \sim t_n(T_n/T_i)^{1/2}$, where t_n represents the time-scale for the neutral gas.

Adopting the values $r_0 = 10^{15}$ cm, $N_H = 10^6$ cm^{-3} (see Section 3.1), $T_n = 10$ K and $T_i = 10^4$ K (Dyson *et al.* 1989), we find that for the superwind, with a mass-loss rate of $\simeq 10^{-5}\,M_\odot$ yr^{-1}, $n_w \sim 10^2$ cm^{-3} and $v_w \sim 25$ km s^{-1}:

$t_n \sim 10^3$ yr and $t_i \sim 40$ yr.

Similarly, for the fast wind, with a mass-loss rate of $10^{-8}\,M_\odot$, $n_w \sim 10^{-4}$ cm^{-3} and $v_w \sim 2000$ km s^{-1}:

$t_n \sim 10^4$ yr and $t_i \sim 400$ yr.

As the superwind lasts for $\sim 10^3$ yr and the fast wind for $\approx 10^4$ yr, either one is capable of pulling the ionized gas (along with the dust) away from the neutral globule to form the dusty ionized tail that is observed.

This requires, of course, that a significant volume of gas is initially ionized. The depth of ionized gas which can be sustained by the radiation of the central star is

$$\delta r_i \approx \frac{S_*/4\pi R^2}{\beta n_i^2},$$

where S_* is the flux of ionizing photons from the star and R the distance of the clump from the star. β is the recombination coefficient of hydrogen to all but the ground level. The time required to ionize this layer of gas can be shown to be of the order $t_{ion} \sim \delta r_i / c_s$, where c_s is the sound speed of the ionized gas, around 10 km s^{-1} for a temperature of 10^4 K. Adopting the value of $S_* = 3.5 \times 10^{45}$ s^{-1} from Dyson *et al.* (1989) gives $\delta r_i \sim 10^{16}$ cm and $t_{ion} \sim 400$ yr for a globule lying 0.1 pc from the star. The volume of ionized gas is thus comparable to that of the neutral globule, and if it is assumed that the globules were at their present position when the superwind commenced, there would be sufficient time to ionize the layer before the wind reached the globules, as this would take $\approx 10^3$ yr.

The conclusion is that a significant ionized skin can form around the neutral globules and be dragged off in a time shorter than the lifetime of the central star winds. Hence the observed globule tails could be dusty, ionized plasma released by the globule rather than just the effects of shadowing of the stellar radiation. An additional effect, not considered here, which may be important to the consideration of the lifetime of the globules, is radiation pressure on the dust.

ACKNOWLEDGMENTS

DT acknowledges support from the Royal Society through the European Visiting Fellowship Scheme.

REFERENCES

Acker, A., 1978. *Astr. Astrophys. Suppl.*, **33,** 367.
Bohlin, R. C., Savage, B. D. & Drake, J. E., 1978. *Astrophys. J.*, **224,** 132.
Cahn, J. H. & Kaler, J. B., 1971. *Astrophys. J. Suppl.*, **22,** 319.
Capriotti, E. R., 1973. *Astrophys. J.*, **179,** 495.
Daub, C. T., 1982. *Astrophys. J.*, **260,** 612.
D'Odorico, S., 1990. *ESO Messenger,* **59,** 59.
Dyson, J. E., Hartquist, T. W., Pettini, M. & Smith, L. J., 1989. *Mon. Not. R. astr. Soc.*, **241,** 625.
Eckert, W., Hofstadt, D. & Melnick, J., 1989. *ESO Messenger,* **57,** 66.
Gull, S. F., 1989. In: *Maximum Entropy and Bayesian Methods,* p. 53, ed. Skilling, J., Kluwer, Dordrecht.
Hildebrand, R. H., 1983. *Q. J. R. astr. Soc.*, **24,** 267.
Huggins, P. J. & Healey, A. P., 1986. *Astrophys. J. Lett.*, **305,** L29.
Kirkpatrick, J. P., 1972. *Astrophys. J.*, **176,** 381.
Leene, A. & Pottasch, S. R., 1987. *Astr. Astrophys.*, **173,** 145.
Meaburn, J. & White, N. J., 1982. *Astrophys. Space Sci.*, **82,** 423.
Nittman, J., Falle, S. A. E. G. & Gaskell, P. H., 1982. *Mon. Not. R. astr. Soc.*, **201,** 833.

Seaton, M. J., 1979. *Mon. Not. R. astr. Soc.*, **187,** 73P.
Skilling, J., 1989. In: *Maximum Entropy and Bayesian Methods,* p. 45, ed. Skilling, J., Kluwer, Dordrecht.
Storey, J. V. W., 1984. *Mon. Not. R. astr. Soc.*, **206,** 521.
Vorontsov-Velyaminov, B. A., 1968. In: *Planetary Nebulae, IAU Symp. No. 34,* p. 256, eds Osterbrock, D. E. & O'Dell, C. R., Reidel, Dordrecht.
Van Blerkom, D. & Arny, T., 1972. *Mon. Not. R. astr. Soc.*, **156,** 91.
Walsh, J. R. & Meaburn, J., 1987. *Mon. Not. R. astr. Soc.*, **224,** 885.